AUT Journal of Electrical Engineering
10.22060/EEJ.2026.25661.5977

Design and Development of a Bridgeless PFC Active Boost Rectifier for High-Efficiency Wireless Power Transfer

Jothippriya Nachimuthu[1*], Namasivayan Gunasekaran[2], Kalal Muralidhar Goud[3], Rangasamy Sankar[4]

[1*]Assistant Professor, Department of Electrical and Electronics Engineering, Erode Sengunthar Engineering College, Erode, Tamil Nadu, India.
[2]PG scholar, Department of Electrical and Electronics Engineering, Erode Sengunthar Engineering College, Erode, Tamil Nadu, India.
[3]Assistant Professor, School of Technology, Woxsen University, Telangana-502345, India.
[4]Professor, Department of Electrical and Electronics Engineering, Chennai Institute of Technology Chennai- 600069, Tamil Nadu, India.

*Corresponding author E-mail: [1]jothippriyan@gmail.com

Abstract:

Wireless power transfer (WPT) enables the transmission of electrical energy without physical connections, commonly used in charging devices and electric vehicles. Conventional methods often face limitations including narrow range, inadequacies in energy transfer, and high costs associated with infrastructure. In order to overcome the issues, this research proposes a Bridgeless Power Factor Correction Active Boost Rectifier (PFC-ABR), aimed at enhancing the efficiency of WPT for charging applications. The proposed architecture employs an AC source connected to a source inductance, which transfer power into a Bridgeless PFC-ABR that efficiently converts AC to DC power. The rectified output is processed by a single-phase high-frequency inverter, generating high-frequency AC power that is transmitted wirelessly through an isolation transformer. On the secondary side of the transformer an interleaved synchronous rectifier is provided to obtain a stable DC output, supplying power to the load through a capacitor bank. The experimental results are implemented by using MATLAB SIMULINK software which displays the efficiency as 93% with reduced THD 0.49% along with unity power factor. The proposed framework, demonstrates significant potential towards improving the performance of wireless charging systems, making it highly suitable for future high-efficient and high-power wireless energy applications.

AUT Journal of Electrical Engineering
10.22060/EEJ.2026.25661.5977

Keywords:

AC source, Bridgeless PFC Active Boost Rectifier, Interleaved Synchronous rectifier, Single phase high frequency inverter, PI controller, Capcitor bank

1. Introduction

WPT technology has benefits of safety convenience, electronic isolation, making it a suitable choice for high power applications related to EV, IoT, Bio-medical implants. It is also useful in battery charging systems, by conversion of magnetic energy into electrical energy. It has reduced complexity of WPT, maintains voltage stabilization, reduced power loss, and low cost. However conventional techniques for this WPT faces challenges like: most existing structures are desingned based on simulation, which results in poor misalignment in tolerance [1-3].

The self-excited inverter which improves the transfer efficiency in WPT and used for analyzing power losses. It has high reliability, low maintenance, robustness, and inherrent short-circuit protection and however it has poor voltage, limited power control, and low efficiency. A WPT system, with control algorithm used for EV charging application that enables continuous power transfer, it illustrates good performance, maintain power and voltage across load during transient condition and robustness. However it suffer from high switching losses, less efficiency, high cost and require high number of components [4-6]. However to overcome the drawbacks faced in conventional WPT systems, rectifiers are used for improving the power transfer from AC source to DC source.

A unity power factor rectifier which has low harmonic distortion and it contributes in reduction of conduction losses, reudces number of components, minimizes voltage stress, improves power density, and increases the power factor. However it has few diodes, dynamic fluctuations, poor performance and reliability, compact design and less efficiency [7-8]. Compact microwave rectifier with low power wireless charging applications has effiicent harmonic manipulation, low power consumption, better performance. Nevertheless, the size of the structure is enlarged with weak components and high cost. Microwave retcifier with harmonic termination structure for low power with wireless charging system has better performance, accurate size, low cost, and minimized losses.. However it accurately measures high impedance but only suitable for low frequency applications and has less efficiency [9-10]. An active rectifier with embedded current monitoring capabilities for WPT system, which has stable and robust frequency, additional current monitoring capability under varying load condition. Nevertheless it has overcurrent during transient process, and it faces electromagnetic challenges, with higher hardware cost [11-12]. High efficiency rectifier for WPT in sensor network and dual output regulating rectifier provides more stable and effiicent power supply for sensor networks and WPT applications. The system has high power density, low power fluctuations, and high frequency implementation. However it has increased complexity, additional components is required, high power loss, limited voltage gain [13-14]. T-type rectifier for DC-bus voltage ripple suppression under unbalanced grid condition, the system has reduced voltage ripple, modifies power setpoint, robustness, long-term performance. However the rectifier has reduced circuit power density, high cost and adjustment of capacitors [15-16]. High power rectifier for WPT system determines superior performance, high power handling capacity and exhibits narrow dynamic ranges. But gets limited because of its increase in complexity overall circuit size and increase in number of components [17].

Hence to improve the system performance and to overcome all the limitations the proposed research establishes a bridgeless PFC-ABR for high efficiency WPT system with high frequency inverter. Some of the related works explains the conventional techniques of WPT system.

2. Related Works

Syed Adil Ali Shah *et al* [2025][18] have introduced high efficient cross coupled active rectifier WPT system. It facilitates fast signal processing, rapid response time, significantly reduces leakage current, reduced voltage drop with improved performance. Increased switching losses, unbalanced comparator size and additional components is essential. **Amjad Iqba *et al* [2022][19]** have proposed WPT system for deep implanted bio-medical devices, the system shows a better performance in terms of dual band operation, high power conversion, harvest energy from different sources and recharge the batteries inside the plant. Moreover the operation is inconvenient, costly, and however it suffers from narrow bandwidth.

Fengjiang Wu *et al* [2022][20] have developed dual side closed loop control of WPT with semi active rectifier which ensures stability and greater dynamic performance, feasible, better adaptability. Nevertheless reduction in reliability, power transmission is limited, increased volume, poor control accuracy, decrease in dynamic response speed.

Guangye Li *et al* [2024][21] have presented suppression strategy of rectifier for EV WPT system, because of its simple structure and ease of its implementation. It improves the reliability of equipment operation, steady state power factor, reduced voltage and current impulse. However it faces a large number of harmonics, increased fluctuations.

Vladimir Kindl *et al* [2023][22] have implemented WPT with current doubler rectifier which exhibits higher effiiciency, reduced voltage stress, low cost and lesser complications.However it requires additional switches and passive elements, power loss, load fluctuations.

Chun-Hong Du *et al* [2024][23] have proposed dual band voltage doubler rectifier for WPT applications. It exhibits simple structure and compact structure size, better performance, reduced harmonic suppression. Although it has reduced harmonics but limped elements are lossy at high frequencies and elevate complexity.

Eojin Kim *et al* [2024][24] have developed dual band rectifier based on symmetric impedance control network for high efficient WPT. It has enhanced stability, reduced diode loss, increased risk of diode breakdown. However it has higher voltage stress, increased components, less dynamic response.

10.22060/EEJ.2026.25661.5977

Zbigniew Rymarski *et al* [2024][24] have improved low frequency digital control in voltage source inverter for UPS system which has faster dynamics, less harmonic distortion, fewer oscillations, however it has limited output, poor performance, high switching losses, maximized current ripples.

2-1- Research Gap:

Therefore, no topology currently in use for bidirectional WPT operation concurrently ensures excellent efficiency, decreased harmonic distortion, low voltage stress, and compact structure. For high-efficiency wireless charging applications, this gap drives the developement of a improved gain rectifier that combines shorter conduction paths, better dynamic stability, and higher PQ performance.

2-2- Contribution of proposed work:

- The Bridgeless PFC-ABC is implemented to reduce conduction losses along with a hysteresis current controller for ensuring power factor and improved efficiency.
- A single phase high frequency inverter is used for the conversion of DC into AC and providing high power conversion.
- An isolation transformer is employed to provide galvanic isolation between circuits and it improves power density.
- Interleaved synchronous rectifier reduces the output ripple and enhances the overall efficiency of the system.

2-2- Proposed System Description

The input power is supplied from an AC main source where the output from AC source is transferred into bridgeless PFC-ABR that converts AC supply into regulated DC, while achieving unity power factor and reduces harmonics. The rectifier operation is controlled using dual loop scheme comprising a DC link voltage PI controller with hysteresis based PWM generation. The outer voltage loop of a dual-loop PI controller generates reference current and voltage by comparing the measured values with reference DC

10.22060/EEJ.2026.25661.5977

link voltage. The single phase high-frequency inverter receives the regulated DC output and converts into AC at higher switching frequencies appropriate for effective power transfer. The block diagram of proposed system is fig. 1.

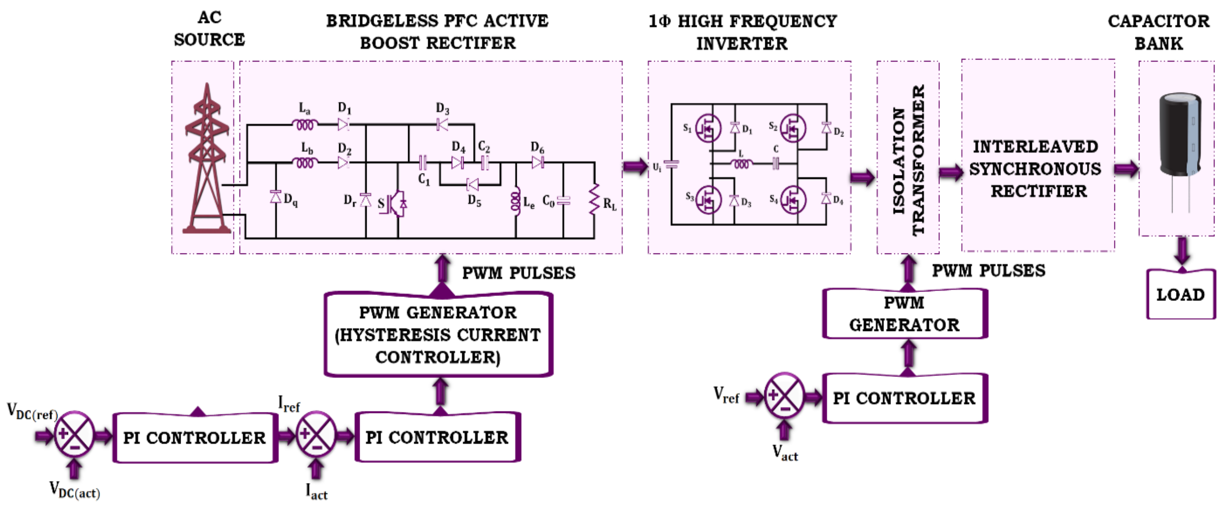

Fig. 1. Block diagram of proposed system

The synchronous rectifier is combined with an isolation transformer for providing galvanic isolation and voltage scaling to meet numerous storage provisions. By using a synchronous rectifier on secondary side which converts high frequency AC converted into DC and a second PI controller generates PWM signals to operate the synchronous rectifier after comparing reference voltage with actual voltage and finally a capacitor bank smooths supplying a stable DC output to the load. Consequently the proposed architecture guarantees effective and adaptable system with improved power factor correction, reduced harmonic distortion, and high efficiency power transfer.

3. Proposed System Modelling

3-1- Bridgeless PFC-ABR

The PFC which act as rectifier which is used to improve the power quality and ensures source voltage and highly essential in WPT and charging system and the proposed circuit includes the parameters of capacitors

10.22060/EEJ.2026.25661.5977

C_1 and C_2 and the inductors as L_a, L_b , low frequency diodes D_1, D_2, D_q, D_r and the high frequency diodes D_3, D_4, D_5, D_6 with an output capacitor C_0. The rectifier works in positive and negative half cycle in line frequency. The circuit is provided in Fig. 2.

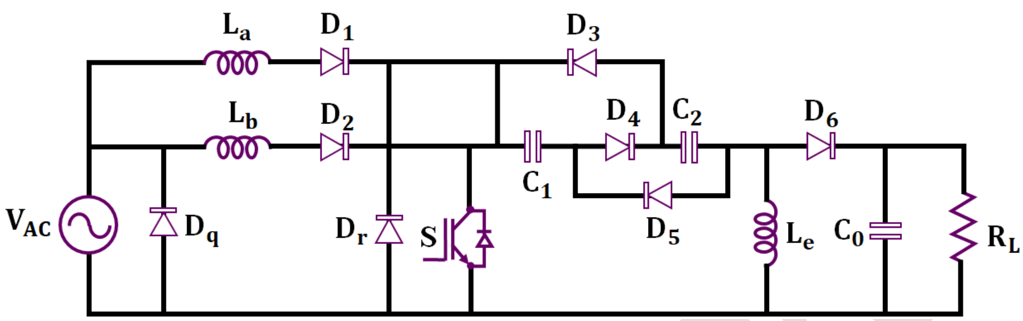

Fig. 2. Equivalent circuit of PFC-ABR

3- 1- 1-The rectifier has two operating modes:

Mode 1: During positive half cycle the switch S turns ON, and the diodes D_1, D_2, D_4, D_6 are active, where the inductor L_a is charged by the input source, and inductor L_c is charged by C_1 and C_2. The circuit for mode 1 is shown in Fig. 3.

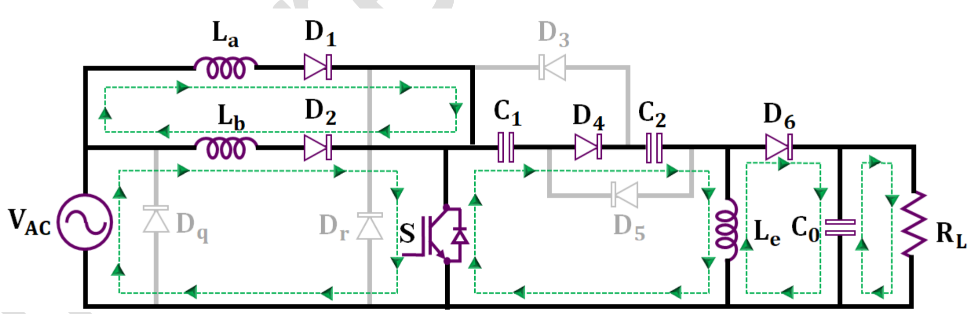

Fig. 3. Mode 1 (SWITCH ON)

The voltage across inductor and capacitor is calculated as,

$$V_{in} = V_{L_a} \tag{1}$$

$$V_{c_1} = V_{c_2} = V_c \tag{2}$$

10.22060/EEJ.2026.25661.5977

Current in the capacitors is equated as,

$$I_{C_1} = I_{C_2} = -\frac{I_{L_e}}{2} \quad (3)$$

$$I_{C_0} = -I_o \quad (4)$$

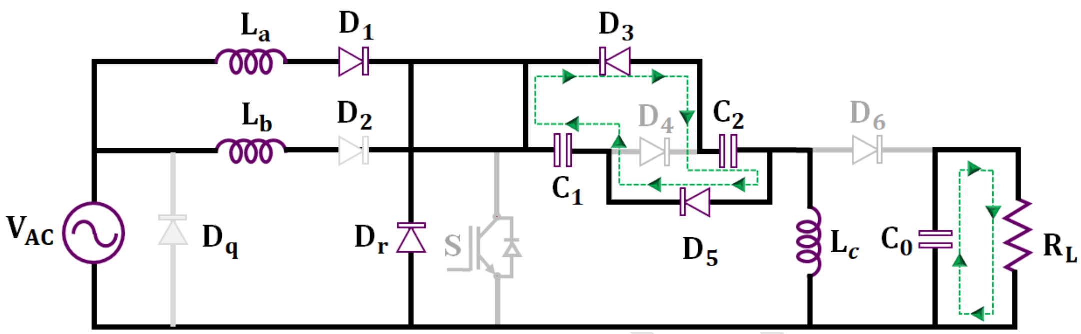

Fig. 4. Mode 2(SWITCH OFF)

Mode 2: When switch S turns off, and the diodes D_r, D_6 are active, where the input voltage is supplied from $V_{ac}$and provides a regulated output voltage across the load resistor R_L through capacitors C_1 and C_2. Mode 2 circuit diagram is exposed in Fig. 4.

Applying KVL around the discharge loop,

$$V_{L_a}^{OFF} = V_{in} - V_c \quad (5)$$

Similarly, for the output-side inductor L_e,

$$V_{L_a}^{OFF} = V_{in} - 2V_c - V_0 \quad (6)$$

Inductor Volt-Second Balance

For $\boldsymbol{L_a}$,

$$\int_0^{T_s} V_{L_a} dt = 0 \quad (7)$$

Or

$$V_{L_a}^{ON} D + V_{L_a}^{OFF}(1-D) = 0 \tag{8}$$

Substituiting,

$$V_{in} D + (V_{in} - V_c)(1-D) = 0 \tag{9}$$

Expanding,

$$V_{in} - V_c(1-D) = 0 \tag{10}$$

Hence,

$$V_c = \frac{V_{in}}{1-D} \tag{11}$$

Output Voltage Derivation

Applying voltage second balance on L_e,

$$V_{L_e}^{ON} D + V_{L_e}^{OFF}(1-D) = 0 \tag{12}$$

Substituiting,

$$V_{in} D + (V_{in} - 2V_c - V_0)(1-D) = 0 \tag{13}$$

Expanding,

$$V_{in} - 2V_c(1-D) - V_0(1-D) = 0 \tag{14}$$

Therefore,

$$V_0(1-D) = V_{in} \tag{15}$$

Hence, the voltage conversion ratio becomes,

$$M = \frac{V_0}{V_{in}} = \frac{1}{1-D} \tag{16}$$

Power Factor Analysis

The input current of a bridgeless PFC rectifier operating in Continuous Conduction Mode (CCM) is regulated to match the waveform of the input voltage.

The instantaneous power is

$$p(t) = v_{in}(t) i_{in}(t) \tag{17}$$

The RMS input power is,

$$P_{in} = V_{in,rms} I_{in,rms} \cos\phi \tag{18}$$

Therefore, power factor is,

$$PF = \frac{P_{in}}{V_{in,rms} I_{in,rms}} \tag{19}$$

For ideal current shaping,

$$i_{in}(t) = I_m \sin\omega t \tag{20}$$

Which is in phase with

$$v_{in}(t) = V_m \sin\omega t \tag{21}$$

Hence, $\phi = 1$ and $PF \approx 1$

Efficiency Analysis

Input and output power is provided as,

$$P_{in} = V_{in,rms} I_{in,rms} \tag{22}$$

$$P_0 = V_0 I_0 \tag{23}$$

Converter efficiency is given as,

$$\eta = \frac{P_0}{P_{in}} \times 100 \tag{24}$$

Substituting

10.22060/EEJ.2026.25661.5977

$$\eta = \frac{V_0 I_0}{V_{in,rms} I_{in,rms}} \times 100 \quad (25)$$

Total power loss is expressed as,

$$P_{loss} = P_{sw} + P_D + P_L + P_C \quad (26)$$

Where, switch conduction and switching losses are represented as P_{sw}, diode losses are P_D, inductor copper or core losses are P_L and capacitor ESR losses are P_C. Hence,

$$\eta = \frac{P_0}{P_0 + P_{loss}} \times 100 \quad (27)$$

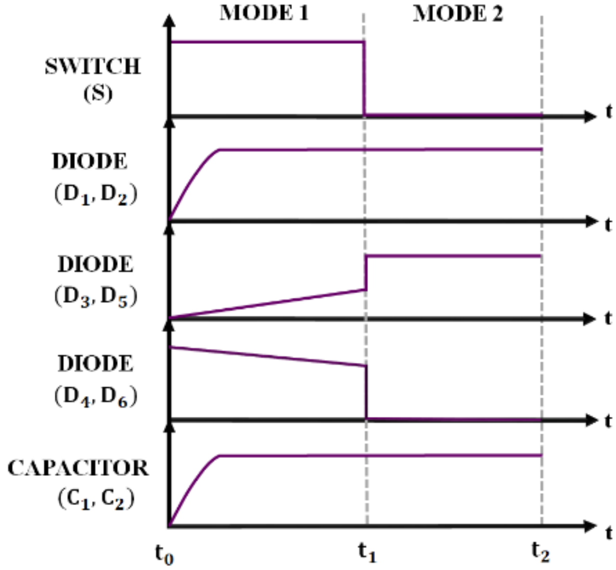

Fig. 5. Switching waveform

Voltage stress across the switches and diodes is indicated as,

$$V_s = 2V_c + V_o \quad (28)$$

Substituting (11),

$$V_s = \frac{2V_{in}}{1-D} + V_0 \quad (29)$$

The switched-capacitor diode experiences capacitor voltage stress,

$$V_c = V_{D3} = V_{D4} = V_{D5} \quad (30)$$

10.22060/EEJ.2026.25661.5977

Fig.5 shows switching waveform of proposed bridgeless PFC rectifier's decreased conduction path reduces diode losses, leading to improved efficiencies under rated operating conditions.

3-2- High frequency inverter

It is an electronic device which converts DC to AC with high switching frequency for achieving high power conversion, and providing a stable output. The LC filter in the inverter ensures a stable and output helps to reduce high frequency noise, reducing harmonic distortion. The circuit diagram for high frequency inverter is shown in Fig. 6.

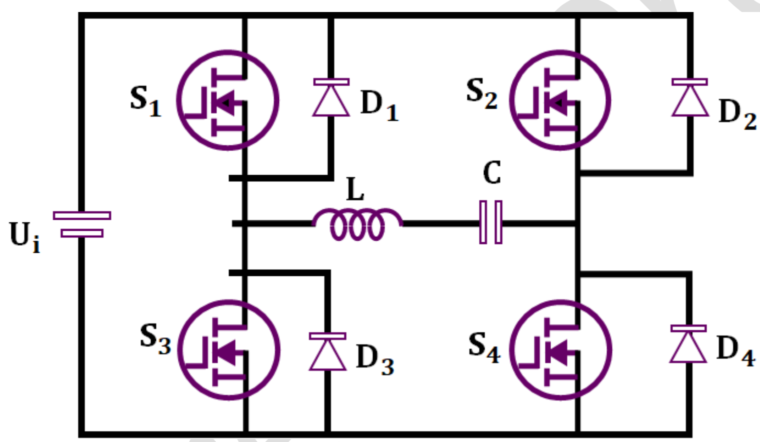

Fig. 6. HF-Inverter

It consist of four parameters as S_1, S_2, S_3, S_4, among the switches S_1, S_2 gets turned ON at the same time and S_3, S_4 turn ON, based on the switches on and off condition the DC voltage is inverted into AC and the reactive power consumption is achieved by series compensation capacitor of primary coil of inverter.

3-3- Isolation transformer

The transformer is used for the conversion of energy specifically related to voltage and current through two windings with numerous turns. The AC power circulating in the primary coil produces magnetic field and magnetic induction gives rises to time-varying magnetic flux circulating in the core. The winding structure is provided in Fig. 7.

10.22060/EEJ.2026.25661.5977

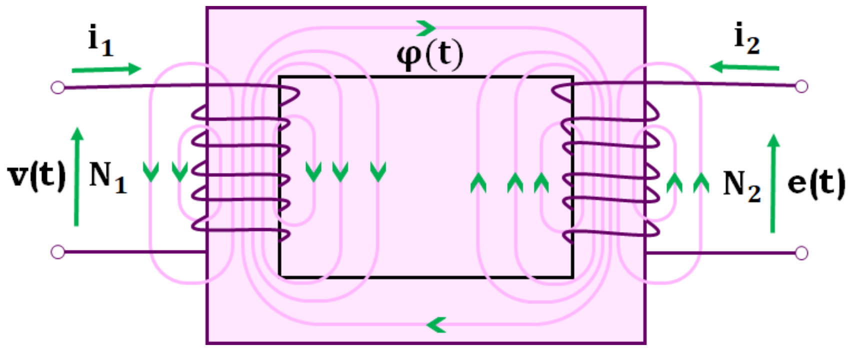

Fig. 7. Basic structure for winding

From the secondary coil, the induced electromagnetic force is generated and the mathematical relation is expressed as,

$$\vec{B}(t) = \mu * \vec{H}(t) \quad (31)$$

$$\varphi(t) = \int_s \vec{B} * \vec{n} ds \quad (32)$$

$$e(t) = -N_2 \frac{d\varphi}{dt} \quad (33)$$

The fundamental function of this transformer is to provide galvanic isolation between windings, and usually the windings are separated by an insulating layer and ensures protection by electrical protection system.

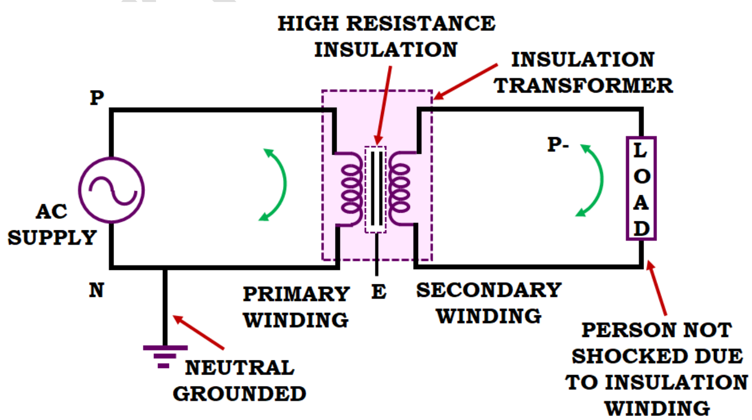

Fig. 8. Isolation transformer

10.22060/EEJ.2026.25661.5977

From Fig. 8 neutral line is connected to ground without interconnecting the windings and therefore the necessity of electrical shock is neglected and human beings touches the supply are easily isolated from the main supply. Subsequently a synchronous rectifier converts AC to DC which is frequently supplied to the capacitor bank.

3-4- Interleaved synchronous rectifier

An interleaved synchronous rectifier is an advanced power conversion topology which combines interleaving and synchronous rectification. It is used for stepping down high voltage and replace diodes with active switches in order to reduce output voltage ripple. This rectifier is revolutionized with power conversion and improved efficiency, while conventional techniques relay on other diodes, normally the forward voltage drop across rectifier in series with output voltage and the gate drive signal is the calculating factor for efficiency gain. It converts the AC power from transformer into DC and the output voltage from this rectifier is sensed using PI controllers, the upper half of secondary winding is positive and current is conducted to the output by operating the switches.

4. Result and Discussion

This section deliberates overall results gained from MATLAB/Simulink of proposed system for PFC-Active Boost Rectifier with capacitor bank assessment in high efficiency WPT. Additionally, the investigation is made over with the traditional approaches to expose the significance of proposed work. Following Table 1 illuminates parameter specification for the proposed topology using MATLAB platform.

Table 1. Parameter specification

Parameter	**Rating**
Source voltage	$350V$
Source current	$75A$
PFC- active boost converter	
Switching frequency	$10kHz$
Inductor L_a, L_b, L_c	$4.7mH$
Capacitor C_1, C_2	$22\mu F$
Capacitor C_0	$2200\mu F$

AUT Journal of Electrical Engineering
10.22060/EEJ.2026.25661.5977

CASE 1: AT 230V

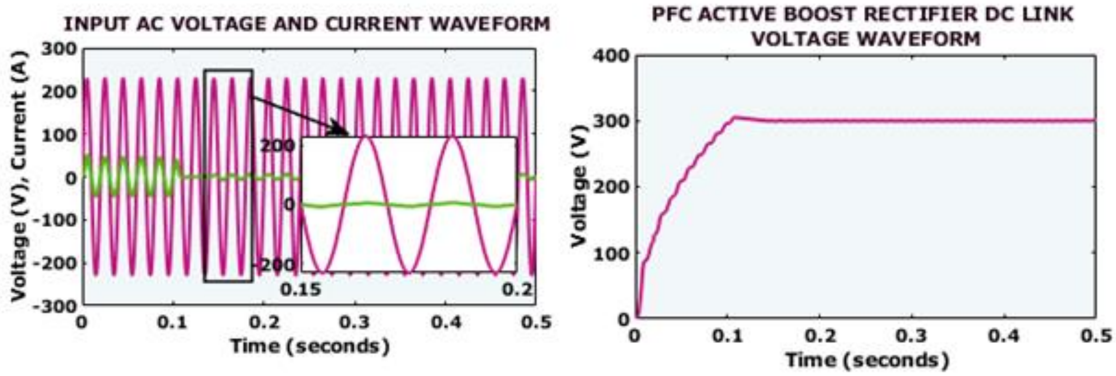

Fig. 9. Input AC waveform and Proposed rectifier DC-link waveform

Fig. 9 shows the input waveform of AC voltage and current and proposed rectifier voltage waveform. The Input AC source voltage has a higher amplitude than the current and both are roughly in phase. The voltage peaks approximately at $230V$ and current peaks approximately $30A$ indicating power factor closely to unity. The proposed rectifier voltage attained by the rectifier is $300V$ over $0.5s$ of its time period with a settling time of $0.1s$ respectively.

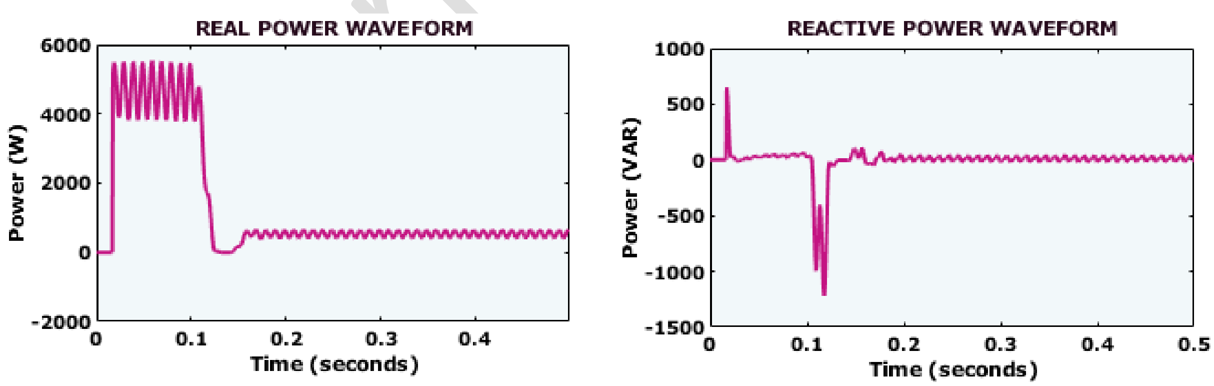

Fig. 10. Real and reactive power waveform (Case 1- 230V)

Fig. 10 indicates the real and reactive power waveform. The waveform of real power showing a high power demand at $0.15s$ and substantially reactive power provides a significant spikes during high power demand

AUT Journal of Electrical Engineering
10.22060/EEJ.2026.25661.5977

phase indicating reactive power compensation, after 0.15s the reactive power stabilizes to null value suggesting more efficient power factor in steady state.

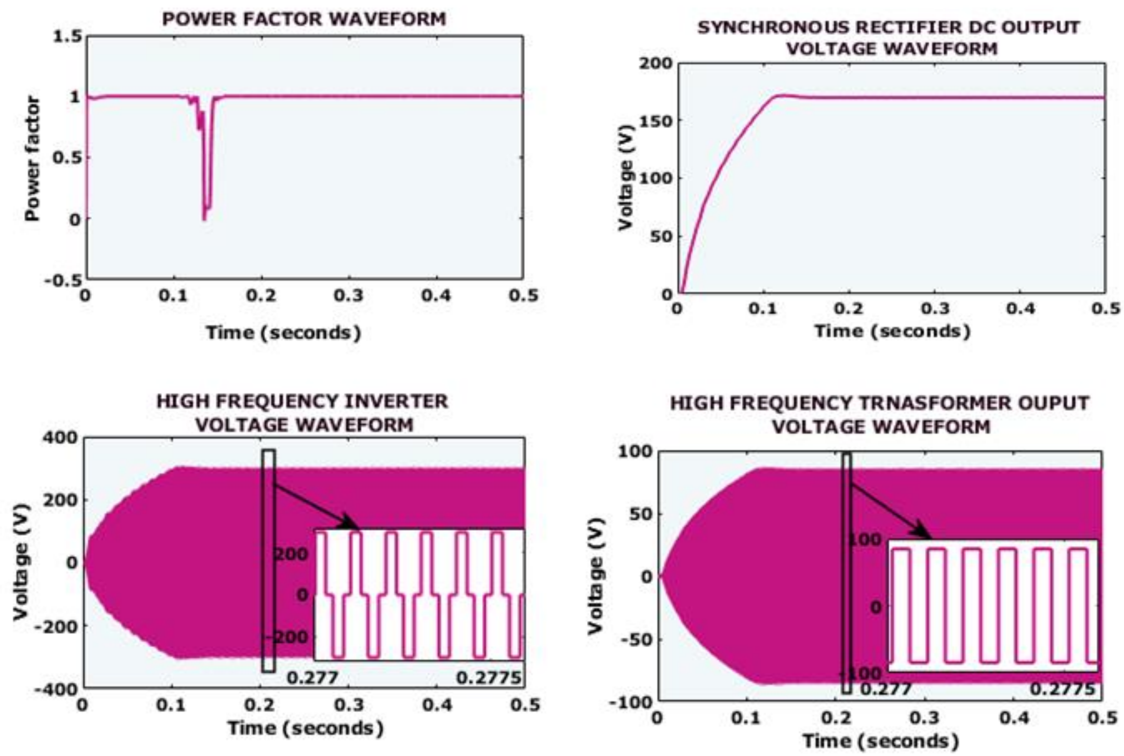

Fig. 11. Power factor, Synchronous rectifier, High frequency inverter and transformer voltage waveform (Case 1- 230V)

Fig. 11 represents the PF waveform, synchronous rectifier, high frequency inverter and transformer output waveform. The achieved power factor is unity and generally stable, a peak temporary drop in power factor occurs approximately $0.14s$. Thus the unity power factor defines the system's stabilized performance. The synchronous rectifier output voltage has achieved $170V$ approximately where it rapidly increases and stabilized at constant level after $0.15s$. High frequency voltage waveform showing the voltage ranges around $400V\ to - 400V$ along with 0 .5s of its time period. The transformer waveform shows the voltage from the transformer as it increases promptly to a steady state voltage approximately $\pm 80V$ at $0.2s$.

10.22060/EEJ.2026.25661.5977

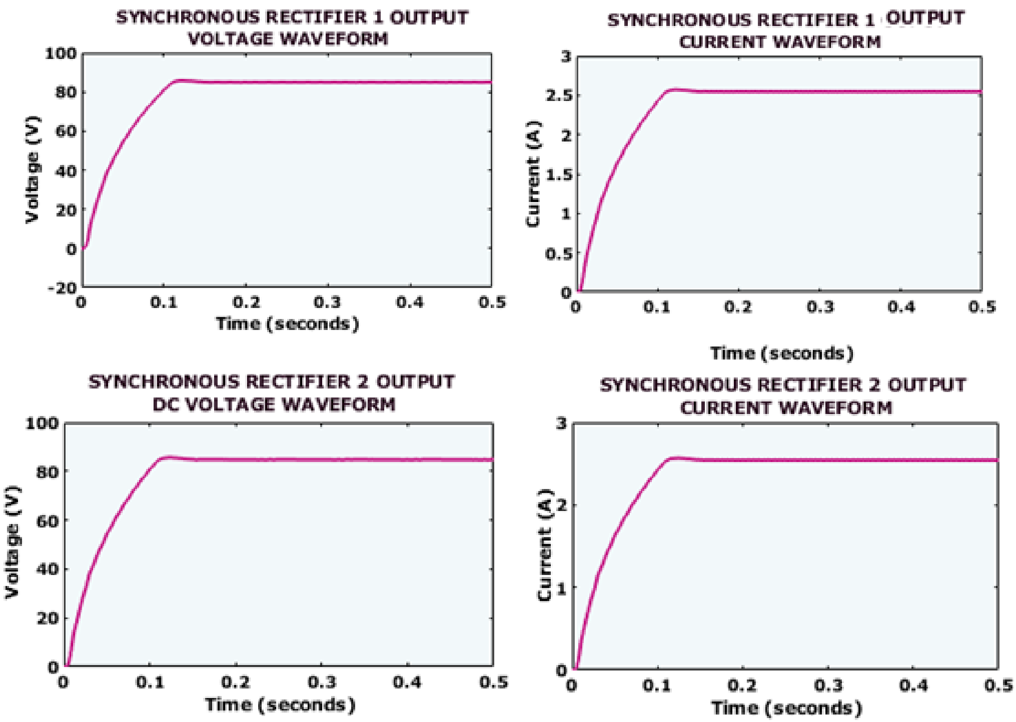

Fig. 12. Synchronous rectifier 1 and 2 waveform output characteristics (Case 1- 230V)

The synchronous rectifier 1 and 2 output characteristics is presented in Fig. 12. The output voltage of rectifier 1 has achieved steady state voltage of $84V$ and the output current is nearly $2.6A$, both the voltage and current reaches its steady state values at 0.15s with less overshoot. The synchronous rectifier 2 showing the achieved output voltage range of $85V$ at 0.2s and the achieved output current approximately $2.5A$ at 0.1s with stable transient response and steady state conditions.

CASE 2: AT 220V

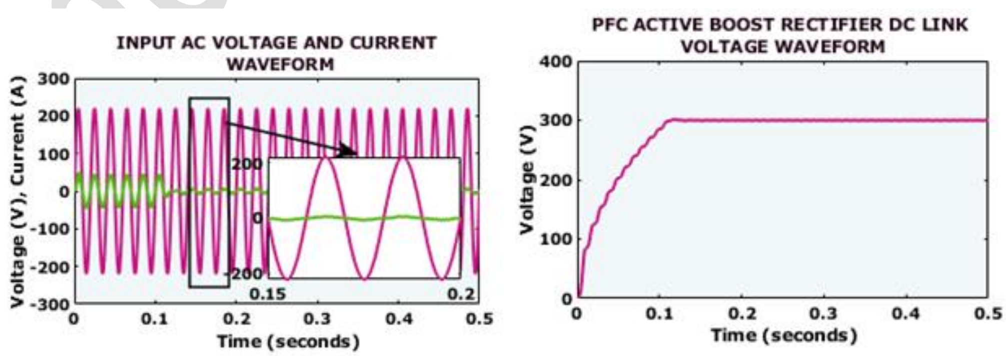

Fig. 13. Input AC sourve nd Proposed rectifier voltage waveform (Case 2- 220V)

10.22060/EEJ.2026.25661.5977

The AC waveform of input current and voltage with rectifier waveform is shown in Fig. 13. The input AC voltage oscillates around $220V$ and current is $30A$ oscillating at a high frequency of 50Hz which appears to be in-phase with the voltage with a duration of $0.5s$ indicating a primarily resistive load. The rectifier waveform shows approximately $300V$to a stable level around $0 to 0.15s$ with a settling time of $0.2s$.

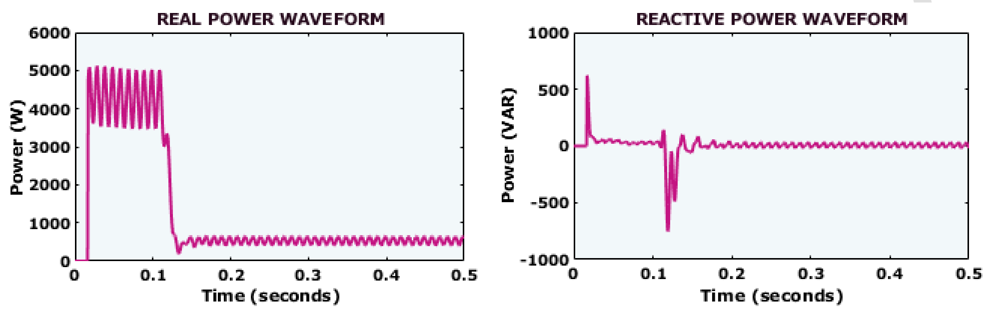

Fig. 14. Power waveform (Case 2- 220V)

The real and reactive power waveform presented in Fig. 14. The real power waveform an initial high power consumption which drops approximately $0.12s$ to a stable level. The reactive power exhibits significantly initial transient and oscillations before settling to null value.

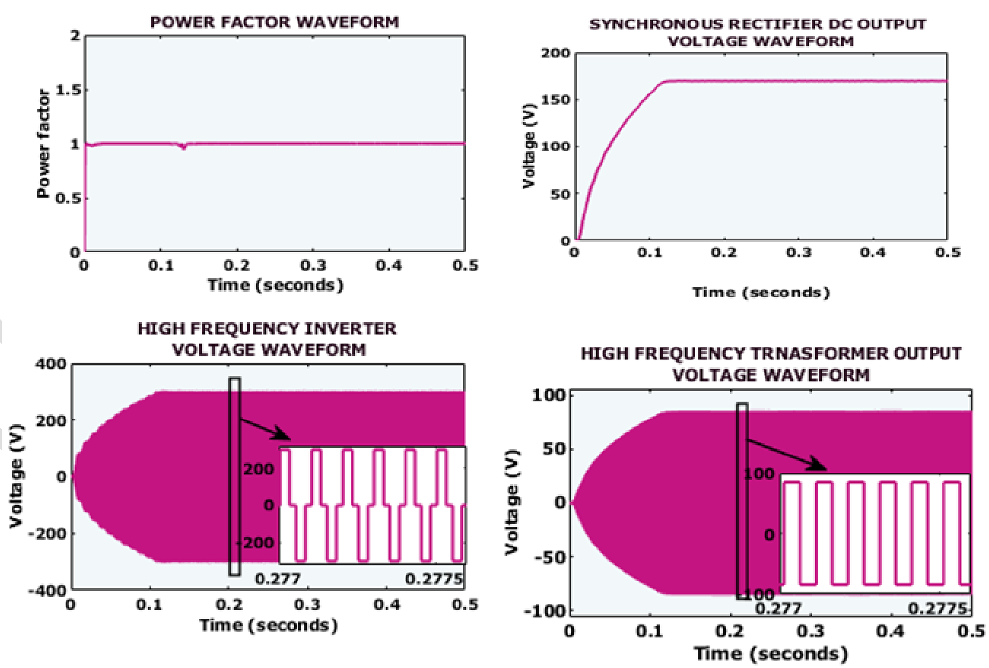

10.22060/EEJ.2026.25661.5977

Fig. 15. Power factor, synchronous rectifier, High frequency inverter, transformer output waveform (Case 2- 220V)

Fig. 15 displays waveform of power factor, synchronous rectifier, high frequency inverter and transformer waveform. The PF quickly stabilizes to 1.0 which remains close to unity power factor ranging from $0\ to\ 0.5s$. The output voltage of synchronous rectifier is $170V$ which rises from 0.1s as startup or transient response to form a stabilized voltage. High frequency inverter voltage starting at zero and rising to a steady state of approximately $300V$ at $0.2s$ which uses high speed switching PWM at magnified view that generates the waveform over 0.5s. The transformer voltage quickly rises to a steady range of $-80V\ to\ 80V$. A magnified pull-out view attentions on a specific time interval between $0.277s\ and\ 0.2775s$, enlightening fast, reliable square wave fluctuations that describe the high frequency operation.

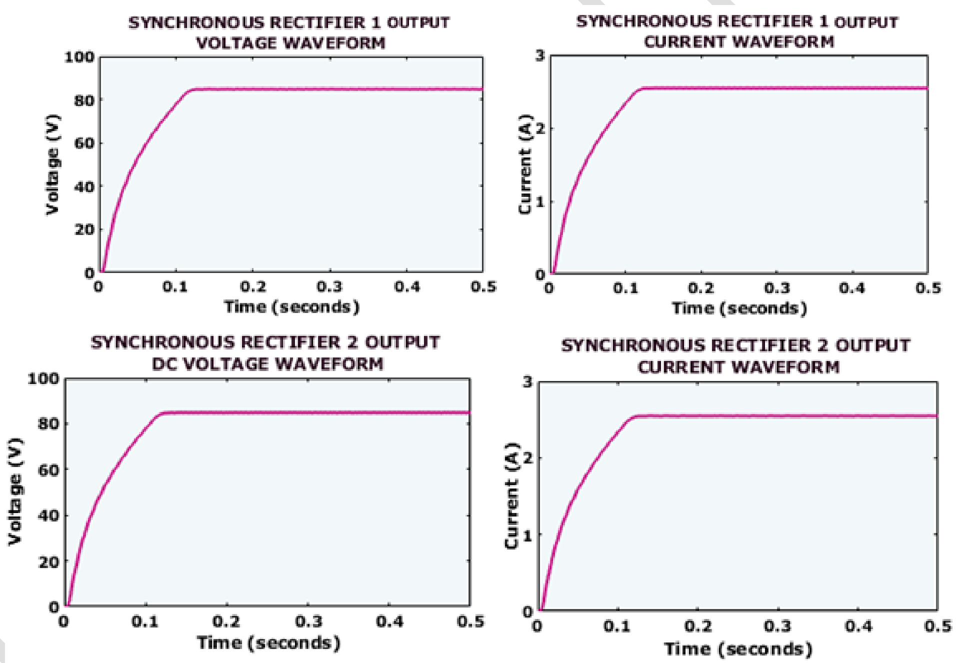

Fig. 16. output waveform of synchronous rectifier 1 and 2 (Case 2- 220V)

The synchronous rectifier 1 and 2 output characteristics is shown in Fig. 16. The output voltage obtained from synchronous rectifier 1 rises around $85V$ at 0.2s and the current attained about $2.8A$ approximately. The synchronous rectifier normally improves efficiency in power conversion circuits, especially for high-current power applications. The output voltage of rectifier 2 has achieved $85V$ with $2.5A$ of output current at $0.15s$. Both the voltage and current waveform stabilizes to reach a stable output with desired time period.

CASE 3: 240V

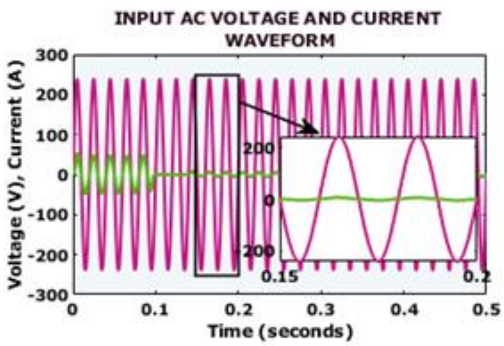

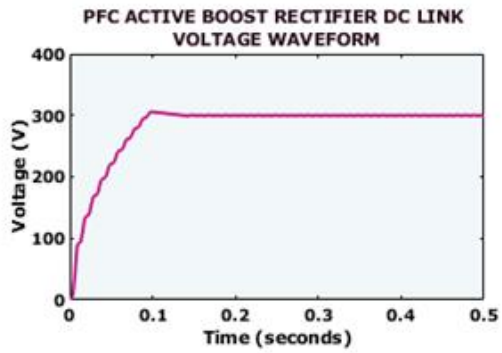

Fig. 17. Input AC source proposed rectifier waveform (Case 3-240V)

The characteristics of input AC voltage and current with proposed rectifier waveform is illustrated in Fig. 17. The input voltage and current which is a sine wave oscillating between $250\ to\ -250V$ and $50\ to\ -50V$ where both waveform changes periodically overtime and the zoomed view highlights large in-phase. The rectifier output voltage starts up with initial fluctuations and approximately stabilized to $300V$ over $0.1s$ and represents the system voltage remains table under further conditions.

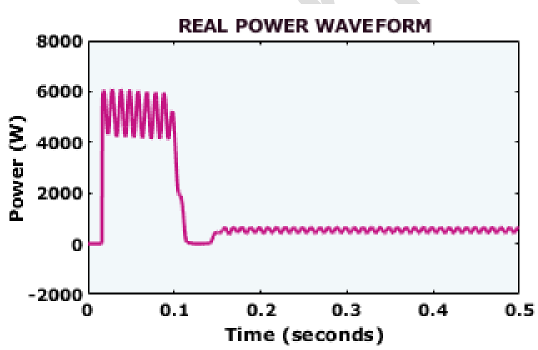

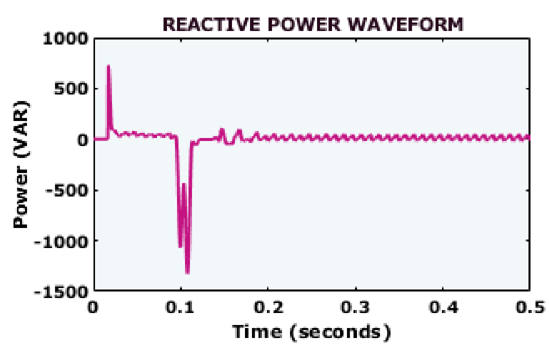

Fig. 18. Waveform of real and reactive power(Case 3-240V)

The real and reactive power waveform indicated in Fig. 18. The real power discriminate initial power consumption approximately 0.1s and the reactive power initiates initial spike before it settling to zero.

10.22060/EEJ.2026.25661.5977

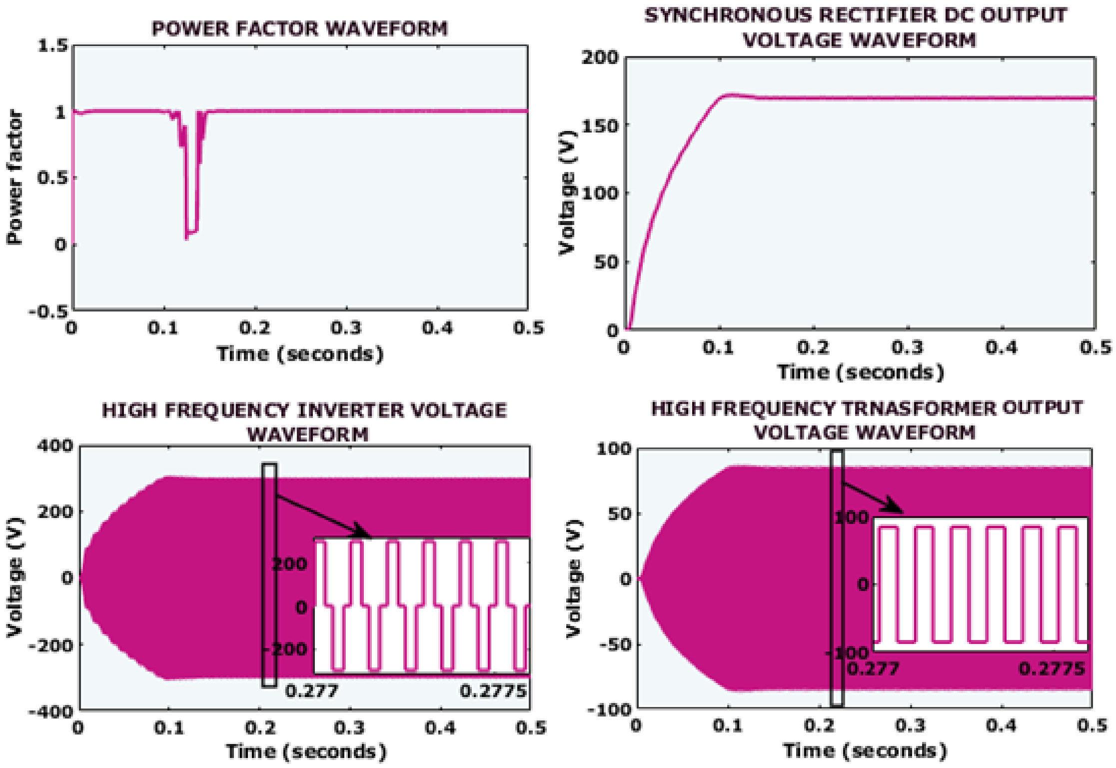

Fig. 19. Power factor,synchronous rectifier, High frequency inverter and transformer waveform (Case 3-240V)

Fig. 19 illustrates waveform of power factor, synchronous rectifier, High frequency inverter and transformer. The system operates with a power factor nearby unity value of time period over$0.5s$. A drop occurs temporarily around $0.12\ to\ 0.15s$. The power factor transitorily drops to zero before improving back to 1.0.This indicates a sudden variation in load. The output voltage waveform of synchronous rectifier stabilizes approximately $170V$ after $0.15s$ over $0.5s$ of time period, and quickly settles down at $0.2s$. The high frequency inverter voltage reaches a steady state nearly $300V$ which stabilizes around $0.1s$. The zoomed view of the inverter showing the attained value of $0.227\ to\ 0.2275$ at 0.2s of its time period. The transformer waveform displays the voltage ranges around $80\ to\ -80V$ exhibiting a high frequency with a stable period viewed from the magnified section at 0.2s developing a stable square form.

10.22060/EEJ.2026.25661.5977

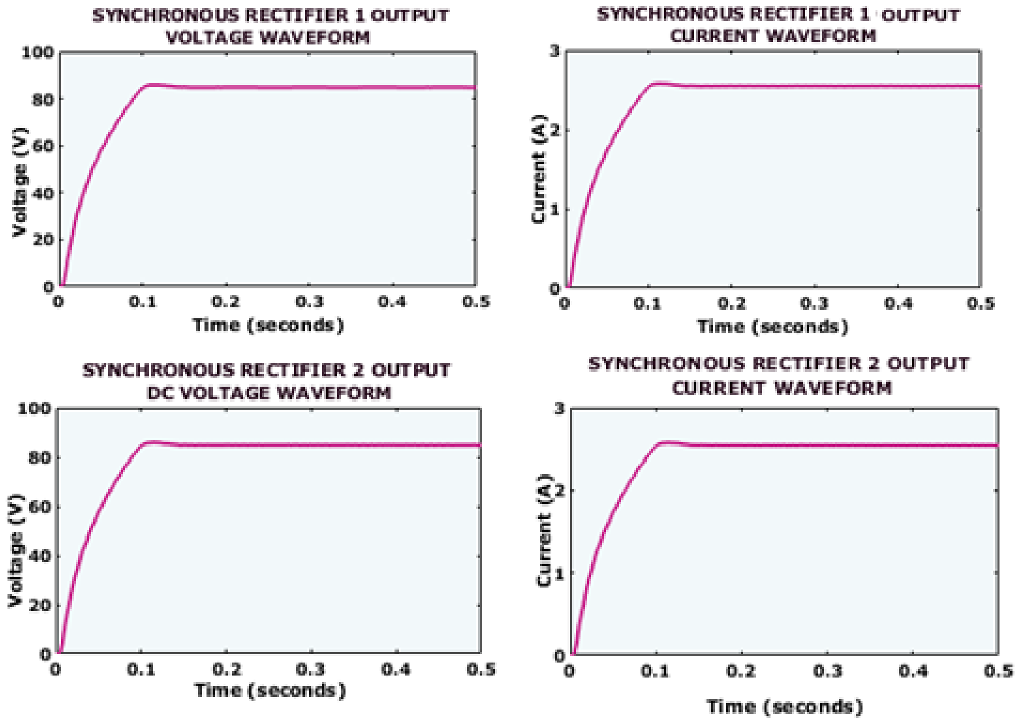

Fig. 20. Synchronous rectifier 1 and 1output

Fig. 20 displays the output of synchronous rectifier 1 and 2 waveforms. The output voltage in the synchronous rectifier 1quickly rises $85V$ stabilizes after $0.1s$. The output current rises to approximately $2.5A$, where both the voltage and current waveform shows a stable output after initial transient period. The output voltage characteristics of rectifier 2 has rapidly rises to $85V$ and stabilizes around $0.15s$. The output current reaches up to $2.5A$ at 0.2s approximately, and reaches a stable value at $0.2s$.

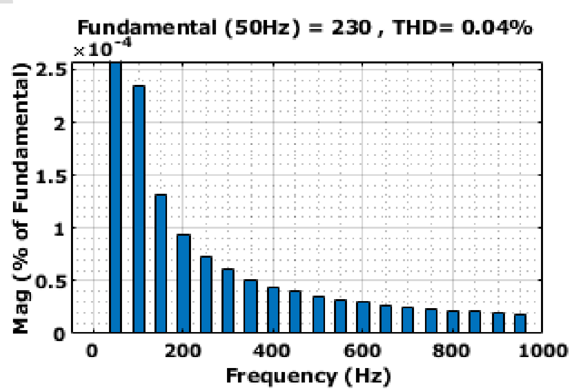

10.22060/EEJ.2026.25661.5977

Fig. 21. THD Waveform

The THD waveform is characterized in Fig. 21. The THD attains a very low value of 0.49% indicating pure sine wave denoting low harmonics with various magnitudes and fundamental frequency of 50Hz.

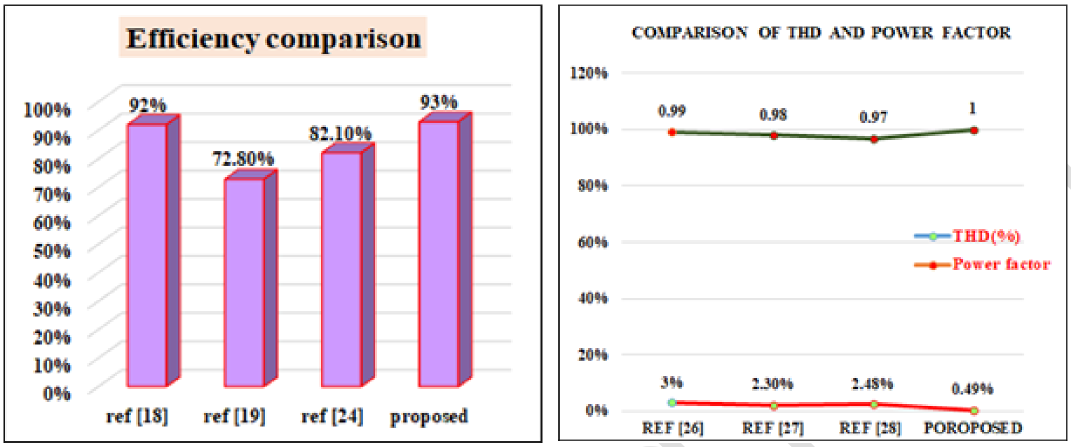

Fig. 22. Comparative analysis of efficiency with PF and THD Comparison

Fig. 22 shows the efficiency with THD and PF comparison. The power conversion efficiency of rectifiers are compared with the proposed rectifier where the rectifier in ref [18] has 92% and ref [19] attains 72.8% similarly in ref [24] 82.1% and the proposed rectifier achieved 93% of power conversion efficiency. The THD attained by other strategies like Ref [26] has 3%, similarly in Ref [27], [28], has 2.3 and 2.48% comparing with proposed method which has reduced THD of 0.49% respectively. PF attained by other rectifiers including Ref [26] has 0.99 PF, similarly in Ref [27], [28], has 0.98 and 0.97 PF and while comparing with proposed rectifier which highly improved as unity PF.

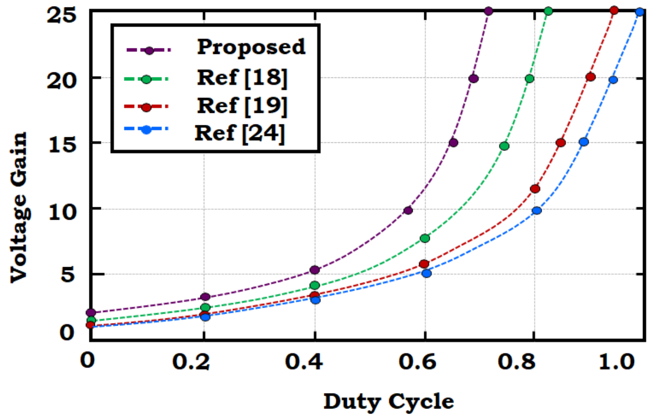

Fig. 23. Voltage gain comparison

Fig. 23 illustrates the voltage gain comparison. The power conversion efficiency of rectifiers are compared with the proposed rectifier where the rectifier in ref [18] and ref [19] ref [24] and the proposed rectifier achieved higher voltage gain.

Table 2. Components comparison

Methodology	Switches	Diodes	Passive components
Proposed	1	8	6
Ref [26]	8	9	7
Ref [29]	2	5	7
Ref [30]	8	4	8

Table 2 describes component comparison. While comparing with other topologies, in Ref [26], [29], [30] the proposed method has less number of components including switches and passive components.

5. Conclusion

The successful implementation of proposed system with bridgeless PFC-Active BR inverter demonstrates significant advancement in WPT system. By integrating PFC-Active BR the system achieves high power factor and exceptionally low THD resulting the system has superior power quality. Furthermore the inclusion of an isolation transformer guarantees safe galvanic isolation between circuits while powering the synchronous rectifier to charge the capacitor bank efficiently. The MATLAB results are verified and the achieved THD level is 0.49% with unity power factor and 93% power conversion efficiency. Consequently the proposed research is crucial for reducing heat generation and exhibits a robust design for advanced efficient wireless charging applications. However, the practical implementation issues will be addressed future research. Hardware prototyping will be used in future work to verify simulation results in real-world scenarios, such as component stress analysis, thermal management, and load variation sensitivity.

References:

[1] X. Yu, J. Feng, L. Zhu, and Q. Li, "Design and optimization of a planar omnidirectional wireless power transfer system for consumer electronics", IEEE Open Journal of Power Electronics, vol. 5, pp. 311-322, 2024.

[2] Z. Yan, C. Hu, B. Hou, and W. Wen, "A Watt-Level RF Wireless Power Transfer System with Intelligent Auto-Tracking Function", Electronics, vol. 14, no. 7, pp. 1259, 2025.

[3] S. Liu, X. Yan, G. Wang, and Y. Liu, "Research on Self-Excited Inverter Rectification Method of Receiver in Wireless Power Transfer System", Processes, vol. 13, no. 1, pp. 89, 2025.

[4] Z. M. Gomes, H. Moussa, Y. Le Gall, E. O. Prado, G. Damm, J. R. Pinheiro, and C. Ripoll, "A nonlinear state-space model and control algorithm for a dynamic wireless power transfer system electric vehicle charger application", Control Engineering Practice, vol. 158, pp. 106270, 2025.

[5] J. Jose, P. Muthukumar, T. Jarin, B. Deepanraj, and M. Sumbwanyambe, "Analysis of L2CL-LCL Based Wireless Power Transfer Compensating System in Electric Vehicle", 2024 International Conference on Futuristic Technologies in Control Systems & Renewable Energy (ICFCR), Malappuram, India, pp. 1-6, 2024.

[6] S. D. Joseph, Y. Huang, and S. S. Hsu, "Transmission lines-based impedance matching technique for broadband rectifier", IEEE Access, vol. 9, pp. 4665-4672, 2020.

[7] W. R. Bennett, Response of a linear rectifier to signal and noise", The Bell System Technical Journal, vol. 23, no. 1, pp. 97-113, 1944.

[8] G. Moloudian, D. R. Gawade, J. L. Buckley, D. Kozlov, S. Bulja, and B. O'Flynn, "A Compact Microwave Rectifier With Class-F Harmonic Termination Structure for Low-Power Wireless Charging Applications", IEEE Sensors Letters, vol. 9, no. 12, pp. 1-4, 2025.

[9] K. Kotani, T. Komiyama, Y. Chonan, and H. Yamaguchi, "Simple Equation-Based Rectifier Model and Its Application to Efficient Energy Harvesting From Amplitude Modulation Broadcasting Radio Waves", IEEE Transactions on Microwave Theory and Techniques, 2025.

[10] S. Lu, and N. Parspour, "Modeling and Design of a Frequency Controller for Full-Bridge Active Rectifier Applied to Wireless Power Transfer System", IEEE Access, 2025.

[11] E. Moisello, A. Gasparini, P. Malcovati, and E. Bonizzoni, "A Novel Active Rectifier With Embedded Current Monitoring Capabilities for Wireless Power Transfer Systems", International Journal of Circuit Theory and Applications, 2025.

[12] Z. Yue, X. Xu, S. H. Wu, and X. Q. Lin, "High-Efficiency and Wide-Dynamic-Range Rectifier Based on Power Reflection for Wireless Power Transfer in Sensor Networks", IEEE Journal of Microwaves, 2025.

[13] T. Lu, and S. Du, "A 92.3%-Efficiency Switching-Mode Dual-Output Regulating Rectifier With Improved Link Adaptability for Wireless Power Transfer", IEEE Journal of Solid-State Circuits, 2025.

[14] Y. H. Liao, J. S. Liu, P. Y. Huang, and P. J. Chen, "Improved Direct Power Control of T-type Rectifiers with Parameter Robustness Feedforward Compensation for DC-Bus Voltage Ripple Suppression Under Unbalanced Grid Conditions", IEEE Open Journal of the Industrial Electronics Society, 2025.

[15] Y. Liu, Z. Guo, F. Liu, F. Guo, K. Wang, Y. Zhu, F. Hou, and X. Wang, "A Real-Time Diagnosis Method of Open-Circuit Faults in Cascaded H-Bridge Rectifiers Based on Voltage Threshold and Current Coefficient of Variation", Electronics, vol. 14, no. 5, pp. 2079-9292, 2025.

[16] X. Yu, J. Zhang, M. Liu, X. Yang, Y. Huang, T. J. Yen, and J. Zhou, "Dual-module ultrawide dynamic-range high-power rectifier for wpt systems", Energies, vol. 17, no. 11, pp. 2707, 2024.

[17] S. A. A. Shah, Y. G. Pu, Y. J. Kim, and K. Y. Lee, "A High Efficient Cross-Coupled Active Rectifier by Using High Speed Switching Comparators for Wireless Power Receiver", IEEE Open Journal of Circuits and Systems, 2025.

[18] A. M. Bhat, and S. Sinha, "A Variable Compensation Rectifier with Enhanced Compensation Capability for Coupling Variations in Wireless Power Transfer Systems", In 2024 IEEE Applied Power Electronics Conference and Exposition (APEC), pp. 1207-1212. IEEE, 2024.

[19] F. Wu, Y. Wei, K. Zhao, and H. Liu, "Dual-side closed-loop control of LCC-S WPT cascaded with secondary semi-active rectifier and controller parameter integrated design", CSEE Journal of Power and Energy Systems, 2025.

[20] G. Li, S. Lv, and R. Yang, "Suppression Strategy of Starting Current Impulse in the Front Stage Rectifier of Electric Vehicle WPT System", World Electric Vehicle Journal, vol. 15, no. 4, pp. 124, 2024.

[21] V. Kindl, M. Zavrel, M. Tyrpekl, M. Frivaldsky, and J. Skorvaga, "Wireless Power Transfer System with Current-Doubler Rectifier on the Secondary Side—Analysis, Modeling, and Verification", Electronics, vol. 12, no. 23, pp. 4818, 2023.

10.22060/EEJ.2026.25661.5977

[22] C. H. Du, F. Cheng, L. Wu, and C. Gu, “Efficient broad dual-band voltage doubler rectifier with multi-section line impedance matching network”, International Journal of Microwave and Wireless Technologies, vol. 16, no. 7, pp. 1133-1137, 2024.

[23] E. Kim, Y. Kim, and J. Oh, “Highly Efficient Dual-Band Rectifier Based on Symmetric Impedance Control Network”, IEEE Access, 2025.

[24] Z. Rymarski, “Improving low-frequency digital control in the voltage source inverter for the UPS system”, Electronics, vol. 13, no. 8, pp. 1469, 2024.

[25] L. Li, Q. Chen, Z. Zhan, and B. Liu, “Multiplexed and Paralleled PFC Rectifier and Its Control”, CSEE Journal of Power and Energy Systems, vol. 11, no. 2, pp. 760-771, 2024.

[26] M. Pourmahdi, H. Heydari-Doostabad, and T. O'Donnell, “A Common Ground Buck-Boost PFC Converter with Quadratic Voltage Gain Ratio and Integrated Active Power Decoupling Capabilities”, IEEE Open Journal of the Industrial Electronics Society, 2025.

[27] F. Yalçın, H. Köse, and A. Savaşcıhabeş, “A Novel IGBT-Based Silicone Carbide Rectifier Design for Improved Energy Efficiency in Telco Data Centers”, Energies, vol. 18, no. 2, pp. 348, 2025.

[28] M. N. Mezaroba, C. H. I. Font, and T. B. Lazzarin, “Single-Phase Voltage-Doubler High-Power-Factor Ćuk Rectifier Operating in Discontinuous Conduction Mode”, IEEE Open Journal of the Industrial Electronics Society, vol. 5, pp. 155-169, 2024.

[29] S. E. Rad, S. Gupta, and S. K. Mazumder, “A Modulation Scheme for Differential-Mode ZVS Resonant-Switched-Capacitor Rectifier”, IEEE Transactions on Power Electronics, 2024.